*Nuclear Society of Slovenia*
2nd Regional Meeting: ***Nuclear Energy in Central Europe***
*Portorož, SLOVENIA, 11.-14.September 1995*



# Second order numerical method for two-fluid model of air-water flow

I. Tiselj, S. Petelin
Institute "Jožef Stefan", University of Ljubljana
Jamova 39, 61111 Ljubljana, Slovenia

**ABSTRACT** - Model considered in this paper is six-equation two-fluid model used in computer code RELAP5. Air-water equations were taken in a code named PDE to avoid additional problems caused by condensation or vaporization. Terms with space derivatives were added in virtual mass term in momentum equations to ensure the hyperbolicity of the equations.

Numerical method in PDE code is based on approximate Riemann solvers. Equations are solved on non-staggered grid with explicit time advancement and with upwind discretization of the convective terms in characteristic form of the equations. Flux limiters are used to find suitable combinations of the first (upwind) and the second order (Lax-Wendroff) discretizations which ensure second order accuracy on smooth solutions and damp oscillations around the discontinuities. Because of the small time steps required and because of its non-dissipative nature the scheme is suitable for the prediction of the fast transients: pressure waves, shock and rarefaction waves, water hammer or critical flow. Some preliminary results are presented for a shock tube problem and for Water Faucet problem - problems usually used as benchmarks for two-fluid computer codes.

## 1. Introduction

Safety analyses of nuclear reactors require computations of complex two-phase flows. Numerical method used in two-phase flow computer code RELAP5 is based upon semi-implicit finite difference scheme with staggered grid and upwind discretization of the convective terms. Method is first order accurate in time and space. Similar scheme is used also in other two-phase flow computer codes. Main advantages of such scheme is its robustness and efficiency while its weak side is numerical dissipation which tends to smear discontinuities on coarse grids.

Second order method presented here was first used to solve gas dynamics equations [1]. We extended the method from three equations to the six equation model of two-phase flow. Due to its accuracy and shock capturing capabilities the scheme is suitable for the prediction of the fast transients: pressure waves, shock and rarefaction waves, water hammer or critical flow.

## 2. Basic Equations

Basic equations taken from RELAP5 are mass, momentum and energy balances for vapour and liquid [2] without terms for interphase mass and heat transfer and wall heat transfer:

$$\frac{\partial(1-\alpha)\rho_f}{\partial t} + \frac{1}{A}\frac{\partial(1-\alpha)\rho_f v_f A}{\partial x} = 0 \qquad (1)$$

$$\frac{\partial \alpha \rho_g}{\partial t} + \frac{1}{A}\frac{\partial \alpha \rho_g v_g A}{\partial x} = 0 \tag{2}$$

$$(1-\alpha)\rho_f \frac{\partial v_f}{\partial t} + \frac{1}{2}(1-\alpha)\rho_f \frac{\partial v_f^2}{\partial x} = -(1-\alpha)\frac{\partial p}{\partial x} + (1-\alpha)\rho_f g\cos\theta - \frac{1}{2}(1-\alpha)\rho_f \frac{f_{w_f}}{D}|v_f|v_f + \frac{C_D}{8}\rho_c a_{gf}|v_r|v_r + CVM \tag{3}$$

$$\alpha \rho_g \frac{\partial v_g}{\partial t} + \frac{1}{2}\alpha \rho_g \frac{\partial v_g^2}{\partial x} = -\alpha \frac{\partial p}{\partial x} + \alpha \rho_g g\cos\theta - \frac{1}{2}\alpha \rho_g \frac{f_{w_g}}{D}|v_g|v_g - \frac{C_D}{8}\rho_c a_{gf}|v_r|v_r - CVM \tag{4}$$

$$\frac{\partial (1-\alpha)\rho_f u_f}{\partial t} + \frac{1}{A}\frac{\partial (1-\alpha)\rho_f u_f v_f A}{\partial x} = -p\frac{\partial (1-\alpha)}{\partial t} - \frac{p}{A}\frac{\partial (1-\alpha)v_f A}{\partial x} + \frac{1}{2}(1-\alpha)\rho_f \frac{f_{w_f}}{D}v_f^2|v_f| \tag{5}$$

$$\frac{\partial \alpha \rho_g u_g}{\partial t} + \frac{1}{A}\frac{\partial \alpha \rho_g u_g v_g A}{\partial x} = -p\frac{\partial \alpha}{\partial t} - \frac{p}{A}\frac{\partial \alpha v_g A}{\partial x} + \frac{1}{2}\alpha \rho_g \frac{f_{w_g}}{D}v_g^2|v_g| \tag{6}$$

Term *CVM* in momentum equations is virtual mass term and is different in RELAP5 than in PDE code. Two additional equations of state for each phase are needed to close the system of equations. Equation of state for phase $k$ is

$$d\rho_k = \left(\frac{\partial \rho_k}{\partial p}\right)_{u_k} dp + \left(\frac{\partial \rho_k}{\partial u_k}\right)_p du_k \tag{7}$$

Derivatives from Eq. (7) can be calculated from the basic thermodynamic relations as:

$$\left(\frac{\partial \rho_k}{\partial p}\right)_{u_k} = \frac{c_{pk}\kappa_k \rho_k - T_k \beta_k^2}{c_{pk} - p\beta_k/\rho_k} \qquad \left(\frac{\partial \rho_k}{\partial u_k}\right)_p = -\frac{\beta_k \rho_k}{c_{pk} - p\beta_k/\rho_k} \tag{8,9}$$

Variables on the right side of the Eqs. (8) and (9) are determined by the RELAP5 water properties subroutines if the pressure and the specific internal energies are known. For metastable states (superheated liquid and subcooled vapour) derivatives in Eq. (7) are determined by extrapolation [2].

Constitutive equations for wall friction and interphase drag were also taken from RELAP5 code. We applied the correlations for the bubbly regime of two-phase flow. In PDE code wall friction terms in momentum Eqs. (3) and (4) were applied in a simplified way comparing to the RELAP5. Our tests showed that this difference did not have a significant influence on the results. The other constitutive equations were applied in the same form as in the RELAP5/MOD3.1.

Virtual mass terms in Eqs. (3) and (4) are coded in RELAP5 with time derivative of the relative velocity only:

$$CVM = C_{vm}\alpha(1-\alpha)\rho_m \frac{\partial v_r}{\partial t} \tag{10}$$

Instead of that difference of the substantial derivatives is suggested to be applied [2]:

$$CVM = C_{vm}\,\alpha(1-\alpha)\,\rho_m\left(\frac{\partial v_g}{\partial t}+v_f\frac{\partial v_g}{\partial x}-\frac{\partial v_f}{\partial t}-v_g\frac{\partial v_f}{\partial x}\right) \tag{11}$$

These form of the derivatives in the virtual mass term was used in PDE code.

Basic RELAP5 equations as coded in RELAP5 present an ill-posed problem [2,3] with complex eigenvalues of the Jacobian matrix (matrix $\underline{C}$ in Eq. (16)). PDE code can solve only well-posed (hyperbolic) problems. With virtual mass term (11) ill-posedness of the equations is avoided for vapour void fractions smaller than approx. 0.7 (Fig. 1). In RELAP5 manual [2], chapter "Special Process Models, Choked Flow" approximate analytical expressions for the Jacobian matrix eigenvalues are found. Results are valid for relative interphase velocity $v_r$ much lower than mixture velocity $v_m$. From these solutions we can see that two approximate eigenvalues contain the term:

$$\sqrt{(\rho_m C_{vm}/2)^2 - \alpha(1-\alpha)\rho_g\rho_f} \tag{12}$$

where $\rho_m$ is two-phase mixture density and $C_{vm}$ is virtual mass coefficient which is in RELAP5 calculated as

$$C_{vm}=\begin{cases}(1+2\alpha)/(2-2\alpha); & \alpha<0.5\\ (3-2\alpha)/(2\alpha); & \alpha>0.5\end{cases} \tag{13}$$

Term (12) becomes imaginary if expression under the root is negative. If Eq. (12) is divided by $\rho_f$ expression (12) can be plotted as a function of $\alpha$ and $\rho_g/\rho_f$. This plot is shown on Fig. 1 where we can clearly see the area of the vapour void fractions and phasic density ratios where RELAP5 equations with complete virtual mass term are still ill-posed.

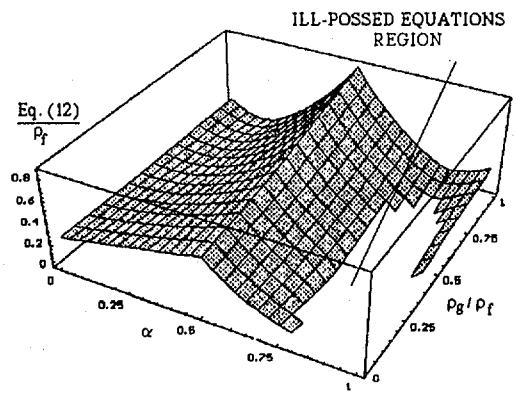


Figure 1: Expression (12) divided by $\rho_f$ with virtual mass coefficient (13) plotted as a function of $\alpha$ and $\rho_g/\rho_f$.

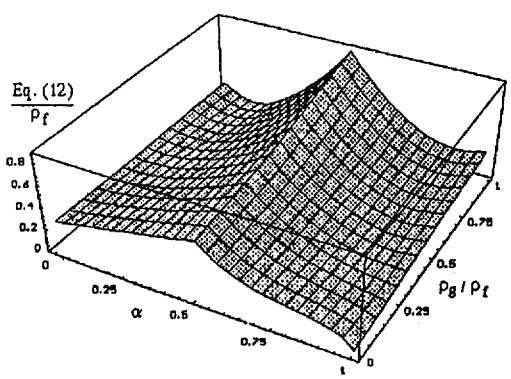


Figure 2: Expression (12) divided by $\rho_f$ with virtual mass coefficient (14) plotted as a function of $\alpha$ and $\rho_g/\rho_f$.

Well-posedness of the equations was ensured with the change of the virtual mass coefficient:

$$C_{vm}=\begin{cases}(1+2\alpha)/(2-2\alpha); & \alpha<0.5\\ \sqrt{\left(\dfrac{3-2\alpha}{2\alpha}\right)^2-\dfrac{(\alpha-1)(2\alpha-1)}{(1+\alpha\rho_g/\rho_f-\alpha)^2}}; & \alpha>0.5\end{cases} \tag{14}$$

In practise this change ensures well-posedness of the equations and does not have any physical

basis behind. To avoid ill-posedness it is necessary to make $C_{vm}$ also a function of the density ratio $\rho_g/\rho_f$. Plot of the expression (12) as a function of $\alpha$ and $\rho_g/\rho_f$ with virtual mass coefficient (14) is presented on Fig. 2.

With virtual mass coefficient (14) PDE eigenvalues were real numbers during all PDE calculations with small and also with large relative interphase velocities. However strict mathematical proof would be needed to show that basic system of equations is well-posed under all types of circumstances where relative velocity $v_r$ is not necessary much smaller than mixture velocity $v_m$.

## 3. Numerical Method

Our program used for solving RELAP5 equations has been named PDE (Partial Differential Equations) and can be used for hyperbolic problems.

System of equations (1)-(6) can be written in the following nonconservative form which is suitable for the numerical solving:

$$\underline{A}\frac{\partial\vec{\psi}}{\partial t}+\underline{B}\frac{\partial\vec{\psi}}{\partial x}=\vec{S}\,, \tag{15}$$

where $\vec{\psi}$ represents the vector of the independent variables $\vec{\psi}=(p,\alpha,v_f,v_g,u_f,u_g)$, $\underline{A}$ and $\underline{B}$ are matrices of the system and $\vec{S}$ is a vector with nondifferential terms in the equations. Equation (15) multiplied by $\underline{A}^{-1}$ from the left gives

$$\frac{\partial\vec{\psi}}{\partial t}+\underline{C}\frac{\partial\vec{\psi}}{\partial x}=\vec{P}\quad . \tag{16}$$

$\underline{C}=\underline{A}^{-1}\underline{B}$ is Jacobian matrix and vector $\vec{P}=\underline{A}^{-1}\vec{S}$. If the eigenvalues and eigenvectors of the matrix $\underline{C}$ are found, Jacobian matrix can be written as

$$\underline{C}=\underline{L}\,\Lambda\,\underline{L}^{-1}\quad , \tag{17}$$

where $\underline{L}$ is matrix of the eigenvectors and $\Lambda$ diagonal matrix of the eigenvalues. If expression for $\underline{C}$ (17) is taken into account in Eq. (16) and equation (16) multiplied by $\underline{L}^{-1}$ from the left we obtain

$$\underline{L}^{-1}\frac{\partial\vec{\psi}}{\partial t}+\Lambda\underline{L}^{-1}\frac{\partial\vec{\psi}}{\partial x}=\vec{R}\quad , \tag{18}$$

where $\underline{L}^{-1}\vec{P}$ has been replaced by $\vec{R}$. Vector of the characteristic variables is introduced as

$$\delta\vec{\xi}=\underline{L}^{-1}\,\delta\vec{\psi}\quad , \tag{19}$$

where $\delta\vec{\xi}$ represents an arbitrary variation: $\partial\vec{\xi}/\partial t$ or $\partial\vec{\xi}/\partial x$. Eq. (16) can be written in the characteristic form

$$\frac{\partial \vec{\xi}}{\partial t} + \Delta \frac{\partial \vec{\xi}}{\partial x} = \vec{R} \quad . \tag{20}$$

Improved characteristic upwind discretization [4] of the Eq. (20) with explicit finite difference scheme is:

$$\frac{\vec{\xi}_j^{n+1} - \vec{\xi}_j^n}{\Delta t} + (\Delta^+)_{j-1/2}^n \frac{\vec{\xi}_j^n - \vec{\xi}_{j-1}^n}{\Delta x} + (\Delta^-)_{j+1/2}^n \frac{\vec{\xi}_{j+1}^n - \vec{\xi}_j^n}{\Delta x} = \vec{R}_j^n \quad . \tag{21}$$

and is first order accurate in time and space [5]. $\Delta^+$ is equal to the matrix $\Delta$ with negative eigenvalues set equal to zero and $\Delta^-$ is equal to the matrix $\Delta$ with positive eigenvalues set equal to zero.

Lax-Wendroff discretization of the Eq. (20) which is second order accurate in space and time is:

$$\frac{\vec{\xi}_j^{n+1} - \vec{\xi}_j^n}{\Delta t} + \Delta_j^n \frac{\vec{\xi}_{j+1}^n - \vec{\xi}_{j-1}^n}{2\,\Delta x} - (\Delta_j^n)^2 \frac{\Delta t}{\Delta x} \frac{\vec{\xi}_{j+1}^n - 2\vec{\xi}_j^n + \vec{\xi}_{j-1}^n}{2\,\Delta x} = \vec{R}_j^n \quad . \tag{22}$$

Problem of the pure second order accurate discretizations are oscillations which appear in the vicinity of the nonsmooth solutions. The problem is solved [1, 6] if the combination of the first and second order accurate discretizations is used. The part of the second order discretization is determined by the so called flux limiters [6] which "measure" the smoothness of the solutions. If the solutions are smooth larger part of the second order discretization is used, if the solutions are nonsmooth larger part of the first order discretization is used.

Final high-resolution shock-capturing discretization of the Eq. (20) with flux limiter $\phi$ is:

$$\frac{\vec{\xi}_j^{n+1} - \vec{\xi}_j^n}{\Delta t} + (\Delta^{++})_{j-1/2}^n \frac{\vec{\xi}_j^n - \vec{\xi}_{j-1}^n}{\Delta x} + (\Delta^{--})_{j+1/2}^n \frac{\vec{\xi}_{j+1}^n - \vec{\xi}_j^n}{\Delta x} = \vec{R}_j^n \quad . \tag{23}$$

where elements of the diagonal matrices $\Delta^{++}, \Delta^{--}$ are calculated as:

$$\lambda_k^{++} = \max(0, \lambda_k) + \frac{\phi_k \lambda_k}{2}\left(\lambda_k \frac{\Delta t}{\Delta x} - \frac{\lambda_k}{|\lambda_k|}\right), \qquad k=1,6 \tag{24}$$

$$\lambda_k^{--} = \min(0, \lambda_k) - \frac{\phi_k \lambda_k}{2}\left(\lambda_k \frac{\Delta t}{\Delta x} - \frac{\lambda_k}{|\lambda_k|}\right), \qquad k=1,6 \tag{25}$$

Flux limiter is calculated using MINMOD formula [6]:

$$\phi_k = \max(0, \min(1, \theta_k)) \quad , \qquad k=1,6 \tag{26}$$

where $\theta_k$ measures the ratio of the left and the right gradient in the grid point $j+1/2$:

$$\theta_{k,j+1/2} = \frac{\xi_{k,j+1-m} - \xi_{k,j-m}}{\xi_{k,j+1} - \xi_{k,j}} \quad , \quad m = \frac{\lambda_{k,j+1/2}}{|\lambda_{k,j+1/2}|} \quad , \quad k=1,6 \quad , \quad j=1,N-1 \tag{27}$$

If Eq. (23) is transformed into basic variables we obtain a difference scheme that is used in PDE code:

$$\frac{\vec{\Psi}_j^{n+1} - \vec{\Psi}_j^n}{\Delta t} + \underline{C}_{j-1/2}^{++} \frac{\vec{\Psi}_j^n - \vec{\Psi}_{j-1}^n}{\Delta x} + \underline{C}_{j+1/2}^{--} \frac{\vec{\Psi}_{j+1}^n - \vec{\Psi}_j^n}{\Delta x} = \vec{P}_j \quad . \tag{28}$$

with

$$\underline{C}_{j-1/2}^{++} = \underline{L}_{j-1/2} \underline{\Delta}_{j-1/2}^{++} \underline{L}_{j-1/2}^{-1} \quad , \quad \underline{C}_{j+1/2}^{--} = \underline{L}_{j+1/2} \underline{\Delta}_{j+1/2}^{--} \underline{L}_{j+1/2}^{-1} \quad . \tag{29}$$

Time step of the scheme is limited with CFL condition $\Delta t \leq \Delta x / \max(|\lambda_k|)$, $k$=1,6.

Integration of the sources is performed in a separated step with second order Euler method. Form of the source term is very important for the behaviour of the equations. In the case of air and water mixture sources are relatively small compared to the convection terms. If system of equations for steam-water mixture is taken into account then sources can be sometimes more important than convection terms. Special treatment of the sources would be required in that case.

Decomposition of the Jacobian matrix (16) has been performed numerically with subroutines from the EISPACK library [7], which are capable to find real or complex eigenvalues and eigenvectors of an arbitrary matrix. PDE program is written only for problems with real eigenvalues of the Jacobian matrix. Calculation is interrupted if complex eigenvalues are found.

Numerical scheme applied in the PDE program is nonconservative scheme. Numerical experiments with the two-phase shock tube problem [6] (closed tube with different initial conditions in each half of the tube) showed practically negligible fluctuations of the overall mass and energy in the tube despite the nonconservative scheme.

## 4. Preliminary Results

PDE code has been used for two numerical benchmarks: two-phase shock tube problem [8] and Water Faucet problem [2].

Tuomi two-phase shock tube problem is a Riemann problem for the two-fluid model with terms for interphase friction neglected. Infinite tube is filled with gas-liquid mixture with the left and right states defined as:

- left state: $\alpha$ =0.25, $p$ =20 MPa, $v_g$ =0 m/s, $v_f$ =1 m/s, $u_g$ =2824 KJ/kg, $u_f$ =1311 KJ/kg
- right state: $\alpha$ =0.1, $p$ =10 MPa, $v_g$ =0 m/s, $v_f$ =1 m/s, $u_g$ =2836 KJ/kg, $u_f$ =1330 KJ/kg

Membrane which separates left and right part of the tube at the position 5 m is removed at time zero. Figures 3 to 6 present comparison of first order characteristic scheme (dotted line) and improvements gained by second order accurate scheme (solid line) on the grid with 300 points. Figure 3 shows the pressure profile at time 0.0056 s with shock wave on the right and rarefaction wave on the left and at time 0.0951 s where the pressure in the observed part of the tube is flat. Void fraction profile on Fig. 4 at time 0.0056 s contains one shock wave, one rarefaction wave and one contact discontinuity. Void fraction on Fig. 4 at time 0.0951 contains three contact discontinuities while the shock and the rarefaction wave at that time stand outside of the observed pipe length. Similar situation can be seen on Fig. 5 for gas velocity. On Fig. 6 where density of the total energy is presented we can see the expected result that solution of the Riemann problem for six equations consists of 7 constant states separated by contact discontinuities, shock waves or rarefaction waves: shock and rarefaction wave are in the observed part of the tube at time 0.0056 s, quasi contact discontinuity at time 0.0056 s in fact contains four waves which are seen at time 0.0951 s.

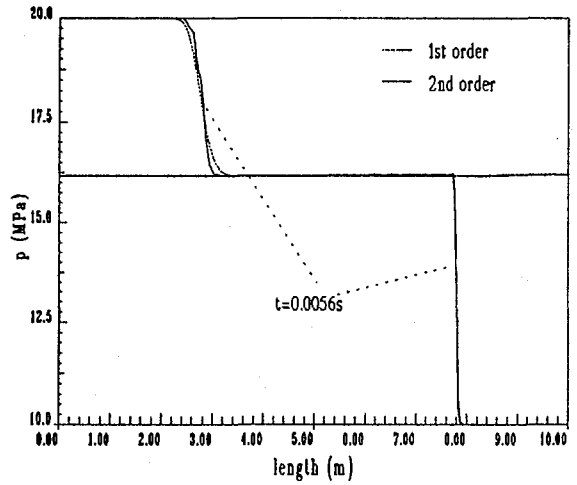


Figure 3: Two-phase shock tube pressure - 1st vs. 2nd order scheme.

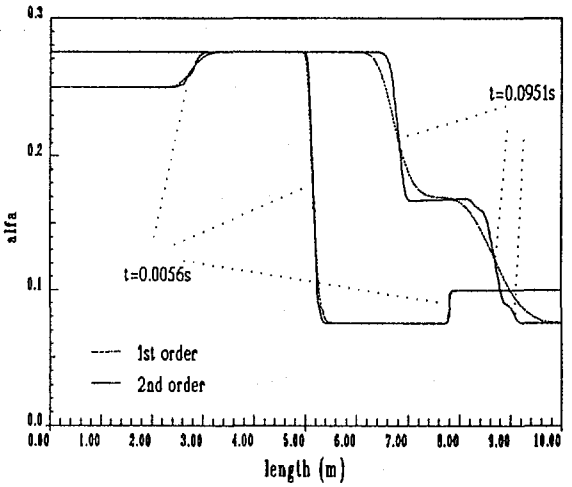


Figure 4: Two-phase shock tube void fraction.

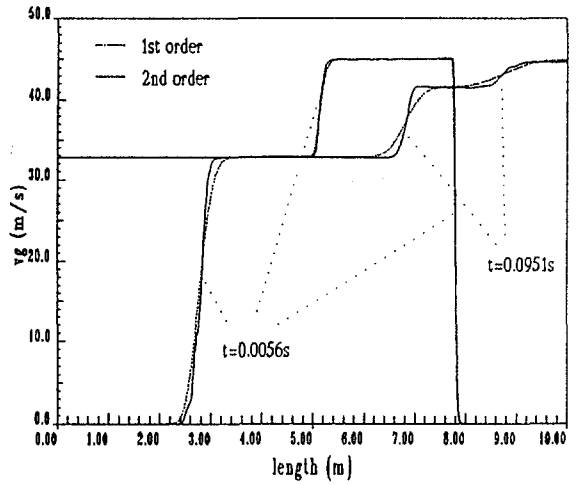


Figure 5: Two-phase shock tube gas velocity.

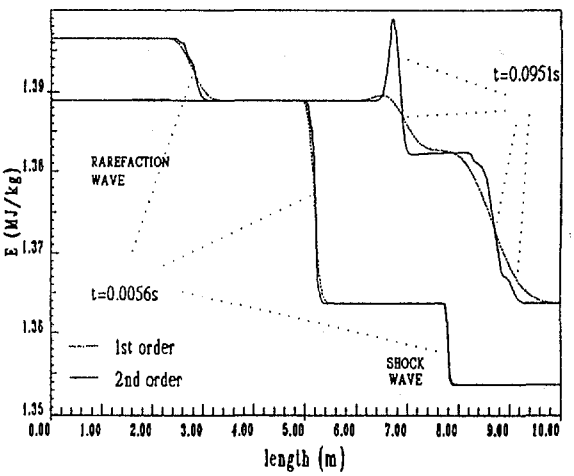


Figure 6: Two-phase shock tube total energy.

Water Faucet problem proposed by Ransom [2] is a vertical water jet inside the cylindrical channel that is accelerated by the gravity. At time zero the pipe is filled with water surrounded by vapour such that the void fraction is 0.2. Liquid column has a uniform velocity 10 m/s and uniform pressure 1 bar. Gas velocity at the beginning is 0 m/s and pressure 1 bar. Specified boundary condition at the inlet is liquid velocity 10 m/s and vapour velocity 0 m/s and constant pressure at the outlet. Analytical solution of the problem exists if interphase and wall drag is neglected. In tests performed by RELAP5/MOD3 code virtual mass term was also turned to zero. In PDE code interphase and wall drag was turned to zero but the virtual mass term had to remain in the code to ensure the well-posedness of the equations. Virtual mass term in PDE code was decreased as much as possible, i.e. it was multiplied by a factor 0.05. At lower multiplication factors equations were ill-posed.

Transient solutions predicted by PDE and analytical solution at time 0.5 s are plotted on Fig. 7. Analytical solution is discontinuous function while the PDE predicts smeared void wave due to the non-zero virtual mass force. Velocity of the PDE void wave is lower due to the same reason. Predicted PDE steady-state void fraction profile which is established after approximately 1 second is equal to the analytical solution.

## 5. Conclusion

High-resolution Shock-capturing method has been successfully applied for the two-fluid model of air-water flow. Results are presented for two-phase shock-tube problem and Water Faucet problem. Further step in the development of the PDE code will be inclusion of the procedure for the handling of the stiff source terms which appear when phase transition is present.

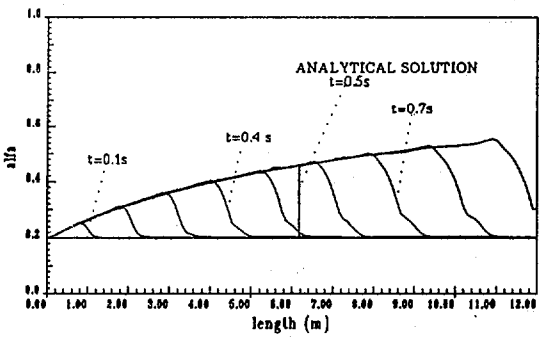


Figure 7: Water Faucet problem. Development of the void fraction profile.

## Nomenclature

$A$ cross section ($m^2$), $a_{gf}$ interphase surface area ($m^2$), $C_D$ coefficient of interphase friction, $c_p$ specific heat capacity at constant pressure (J/kg-K), $C_{vm}$ virtual mass coefficient, $D$ tube diameter (m), $f_w$ wall drag coefficient, $g$ acceleration of gravity (9.81 $m/s^2$), $h$ specific enthalpy (J/kg), $p$ pressure ($N/m^2$), $T$ temperature (K), $t$ time (s), $u$ specific internal energy (J/kg), $v$ velocity (m/s), $x$ space coordinate (m), $\alpha$ vapour void fraction, $\beta$ thermal coefficient of expansion ($K^{-1}$), $\kappa$ isothermal compressibility ($Pa^{-1}$), $\theta$ inclination of the tube, $\rho$ density ($kg/m^3$), $\Lambda, \lambda$ matrix of the eigenvalues, eigenvalue

Subscripts:

$c$ continuous phase, $f$ liquid, $g$ vapour, $i$ interphase surface, $r$ relative (velocity $v_r = v_g - v_f$), $m$ mixture

## References


1. P. L. Roe, "approximate Riemann Solvers, Parameter Vectors and Difference Schemes", J. Comp. Phys. 43, 357-372, 1981.
2. K. E. Carlson, R. A.Riemke, S. Z. Rouhani, R. W. Shumway, W. L. Weaver: "RELAP5/MOD3 Code Manual", Vol. 1-7, NUREG/CR-5535, EG&G Idaho, Idaho Falls, 1990.
3. H. C. No, M. S. Kazimi: "Effects of Virtual Mass on the Mathematical Characteristics and Numerical Stability of the Two-Fluid Model", Nuclear Science and Engineering 89, pp 197-206, 1985.
4. C. Hirsch: :Numerical Computation of Internal and External Flows", Vol 1-2, John Wiley & Sons, 1988.
5. I. Tiselj, S. Petelin: "Verification of the RELAP5 Equations with the Flashing Flow in the Nozzle", FED-Vol.223, Validation of System Transient Analysis Codes, ASME 1995, August 1995, Hilton Head Island.
6. R. J. LeVeque, "Numerical Methods for Conservation Laws", Lectures in Mathematics ETH Zurich, Birkhauser Verlag 1992, Basel.
7. W. H. Press: "Numerical Recipes", Cambridge University Press, 1989.
8. I. Tuomi, "An Implicit Second Order Numerical Method for Two-Fluid Models", ICONE 3, Kyoto, 1995.